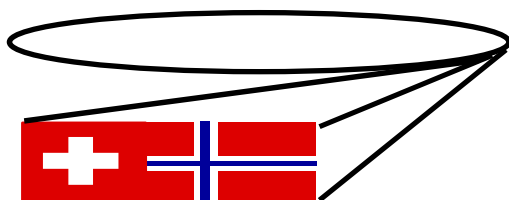




2001

REPORT



The Swiss-Norwegian Beamlines at ESRF

October 2000 – September 2001

IMPRESSUM

SNBL 2001

SNBL 2001 was prepared by Weaver Unlimited for the Swiss-Norwegian Beamlines at ESRF, PO Box 220, F-38043 Grenoble, France

SNBL Director	Hans-Peter Weber	+33 476 88 2396
SNBL Executive Assistant	Chantal Heurtebise	+33 476 88 2615
FAX		+33 476 88 2694
E-mail		ExAsst_snbl@esrf.fr
Website		www.snbl.org

March 2003

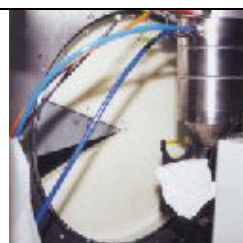
ANNUAL REPORT

OCTOBER 2000 – SEPTEMBER 2001

CONTENTS

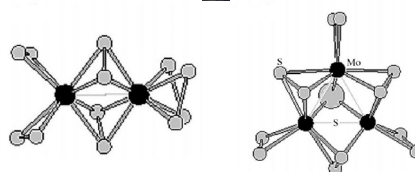
<i>SNBL in Brief</i>	1
<i>Foreword</i>	2
<i>Highlights of 2000-2001</i>	3

Fast Time-resolved *in situ* Powder
Diffraction Studies of High-temperature
Oxidation / Reduction Reactions



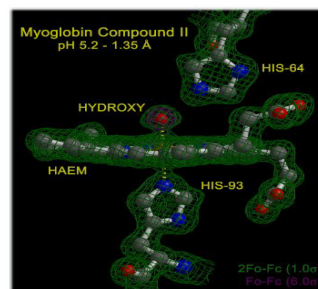
3

QEXAFS Study of the Sulfidation of
NiMo/Al₂O₃ Hydrotreating Catalysts



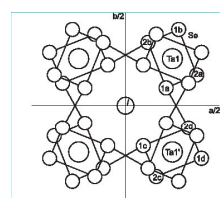
5

Peroxidases: New Resonance Forms
Suggested by pH Dependent Structures
of Intermediates in Myoglobin-Peroxide
Reactions



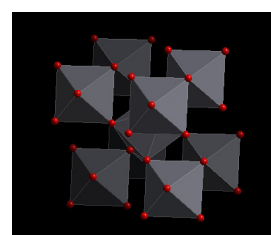
6

Structure of the Charge Density Wave
in (TaSe₄)₂I



7

In-situ Characterization by Raman
Spectroscopy and X-ray Diffraction of
Phase Transitions in Cristobalite under
High Pressure

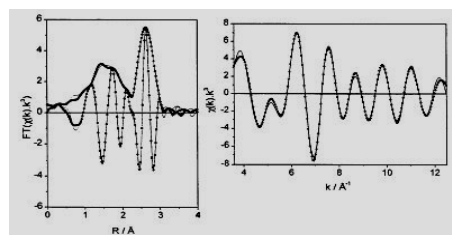


8

Selected Scientific Results

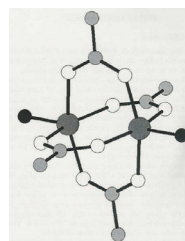
9

Catalysis



9

Novel and Unusual Materials



10

Instrumental Developments

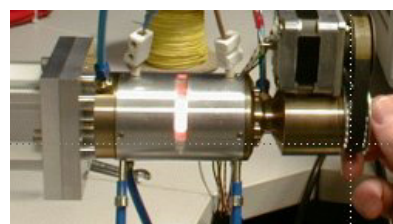
15

Improvement in Flux Density on Beamlines A and B. Part II



15

High-Temperature Furnace for Powder Diffractometry



16

Status of Facility

19

SNBL in Figures

21

Organisational Structure

23

List of SNBL Publications

25

The mission of the Swiss-Norwegian Beamlines at ESRF is to provide scientists from both Norway and Switzerland, from both academia and industry, with increased access to synchrotron radiation and, in particular, state-of-the-art, custom-designed instrumentation for diffraction and absorption experiments. Both partner countries have relatively large and exceptionally active scientific communities using X-ray diffraction and absorption as their main probes; for these groups the amount of public beamtime offered by ESRF was insufficient from day one, and this is the *raison d'être* of the Swiss-Norwegian Beam Lines at ESRF.

Nowadays, it is fully understood by the scientific community that many of the most challenging problems in structural crystallography can be solved only with the use of synchrotron radiation, and even then, often enough, only by harnessing the combined power of two or more experimental techniques (such as, e.g., powder and single-crystal diffraction). The SNBL number four such different experimental techniques, distributed over two beamlines, and presently include:

A. High-resolution single crystal diffractometry

B. Large-area diffraction imaging
C. High-resolution powder diffractometry
D. EXAFS spectrometry

Environmental chambers for extreme conditions (often unavailable in one's home laboratory) complement this equipment and often open up new, previously uncharted terrain.

This unusually broad range of instruments, all available in one facility, is one of the prime strengths of SNBL, a one-stop facility for the solution of complex crystal structural problems. This same broad range is also one of the few weaknesses of the facility: With two beamlines and four experimental techniques, staff needs not infrequently to spend a substantial amount of time to reconfigure the beamlines.

The Swiss-Norwegian Beam Lines are located in Grenoble at the European Synchrotron Radiation Facility, next to the high-flux neutron reactor of the Institut Laue-Langevin. This setting, together with the proximity to several universities and R&D laboratories of international high-technology companies, concur to make Grenoble a pre-eminent pole in solid-state research in Europe and provide a very stimulating working environment for users and staff of the Swiss-Norwegian Beam Lines.

This is the fourth annual report of the Swiss-Norwegian Beamlines (SNBL) at ESRF, the first one having been published in 1997. Reports are issued annually, mid-year, covering a twelve-months period from October to September.

The annual report offers a welcome opportunity for SNBL users and staff alike to appraise what has been achieved, to learn from the past and look to the future, and to decide what ought to be done in the years to come, in short: to develop a proactive vision.

This vision of the future (the next five years) has been the subject of a white paper issued in December 2000 by a select committee of experienced SNBL users, appointed by the steering-and-review committee, and chaired by the SNBL Director. The report discussed mostly the options available to the SNBL as a function of several funding scenarios and sketched a tentative road map for SNBL's future. A copy of this report is to be found on the CD-rom on the back page of this annual report.

As seen from a SNBL user's point of view, the past year (October 2000 – September 2001) witnessed continued successful operation of the facility, the commissioning of several new instruments or instrument upgrades, and a steady increase in usage. All four experimental stations ran as planned, with experiments running in both hutches at all times.

A Powder Diffraction Service has been put into operation and is already attracting a substantial *clientèle*, which seems to appreciate the time-saving it offers. This model may be extended to other techniques -provided additional part-time staff can be found to run the service.

Funding in excess of CHF 1 Mio has been granted to substantially upgrade both the the single-crystal diffractometer and the XAFS branch lines. I anticipate that the

type of experiments using these techniques will become less routine, that these experiments will increase in complexity (we have seen this happen already) and require increased assistance to users. In this context, I would like to encourage users to submit more long-term projects. The process of writing such proposals is likely to stimulate new ideas, a better long-term approach to SNBL and a clearer long-term vision for the future among the staff.

The highlight of 2001, politically speaking, was certainly the decision of the Norwegian partner, the Norsk Synkrotron Forskning A/S, to increase its contribution from ~28% to 50%. This reflects a) the satisfaction of this sponsor in the favorable return on its investment and b) the continuing acceptance by the Norwegian user community of the usefulness of "its" synchrotron.

Finally, the success of the SNBL is not wholly homegrown; it depends heavily on the quality of the beam delivered by the synchrotron radiation facility it is part of. We are fortunate that the performance of the ESRF has been steadily increasing to a peak overall availability of close to 97%. Furthermore, the planned upgrade of the beam current to 300 mA augurs well for yet another growth in experimental possibilities.

In closing, I would like to take the opportunity to thank:

- the backers of the SNBL Project for their generous and continuing support.
- my staff for its unceasing devotion to the project. In a project such as this, the quality of the staff, more than anything else (incl. advanced instrumentation), is the key to its success.

Hans-Peter Weber,

SNBL Director

Fast Time-resolved *in situ* Powder-diffraction Studies of High-temperature Oxidation/Reduction Reactions

P. Norby, H. Fjellvag and H. Emerich

[Oslo and SNBL]

the fast oxidation/reduction reactions of oxygen ion conducting perovskite type materials at high temperature, 400-800°C

The time resolution can be adjusted by varying the slit size and the rotation speed. *In situ* powder diffraction data have been collected with a time resolution around 100 ms.



Fig. 1. The rotating slit system at the MAR345 diffractometer at SNBL. A capillary-based *in situ* micro reaction cell and a hot air heater are mounted on the diffractometer (inset).

In order to perform fast time-resolved *in situ* powder diffraction experiments of chemical reactions, a rotating-slit system for the MAR345 imaging-plate system has been developed for BM01A (SNBL) (Fig. 1). A screen with a wedge-shaped opening is rotated in front of the MAR345 image-plate detector.

The rotating-slit system has been used in time-resolved *in situ* powder diffraction studies of

Perovskite type oxides with composition $(A_{1-x}A'_x)BO_{3\pm\delta}$, ($A = \text{La, Y}$; $A' = \text{Sr, Ca}$; $B = \text{Mn, Fe, Co}$) are of interest for applications such as catalysis, oxygen permeable membranes, solid oxide fuel cells and colossal magneto-resistance. For these materials, catalytic activity, magnetism and oxygen ion conductivity, are closely related to oxygen stoichiometry, crystal structure and redox properties. The oxidation/reduction reactions are of topotactic nature and are completed

within a few seconds at 800°C. Therefore, very fast data collection is required. High-quality powder diffraction data must be collected in order to monitor structural changes during the reaction, preferable by means of Rietveld analysis.

A capillary based micro reaction cell, allowing a flow of gas to pass through the sample, was used for the experiments. Using a remote-controlled three-way valve, abrupt changes between nitrogen and oxygen gas can be achieved, allowing kinetic information to be extracted from variation of intensity or position of selected Bragg reflections. Samples were contained in 0.7-1mm quartz glass capillaries mounted in a Swagelok fitting. The sample was heated using a hot air blower.

Results are presented for oxidation of $\text{SrFe}_{0.97}\text{Cr}_{0.03}\text{O}_{2.6}$ at 700-800°C. Switching from a nitrogen to an oxygen atmosphere is done while the slit is rotating continuously in front of the imaging plate (one rotation in 15 seconds).

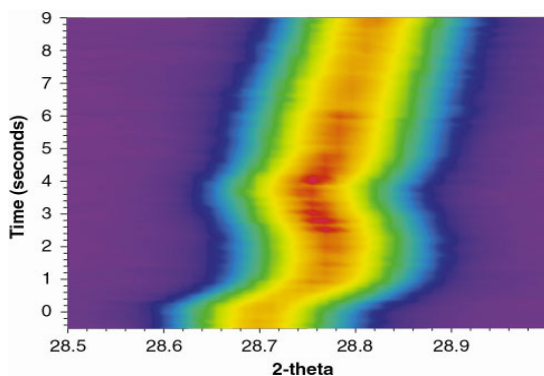


Fig. 2. Changes in position and intensity of one diffraction peak during oxidation of $\text{SrFe}_{0.97}\text{Cr}_{0.03}\text{O}_{3.5}$ at 800°C.

Fig. 2 shows the changes in one of the reflections as the oxidation proceeds at 800°C.

The gas flow was switched from N_2 to O_2 at time $t = 0$, and powder diffraction data were integrated to provide a time resolution of 100 ms. An almost instantaneous change in the diffraction pattern was observed.

The unit cell volume normally decreases during the oxidation of perovskite oxides. This is caused by shortening of the metal-oxygen bond on increased valence state of the cation, together with the efficient packing of coordination polyhedra.

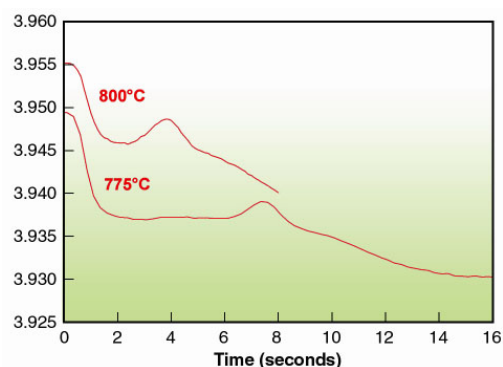
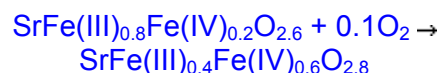


Fig. 3. Unit cell parameter (pseudo cubic) of $\text{SrFe}_{0.97}\text{Cr}_{0.03}\text{O}_{3.5}$ during oxidation at 775 and 800°C.

As an example, consider the oxidation of $\text{SrFeO}_{2.6}$:



Typically the unit cell decrease mirrors the variation in oxygen stoichiometry. For the present oxidation process, the time-resolved data reveal an unexpected increase in the pseudo-cubic unit cell parameter (using LeBail profile refinement) for an intermediate time interval (Figure 3). It can be clearly seen that the oxidation process proceeds in two steps. After an initial fast decrease, a plateau is reached, most visible at 775°C. A maximum in the unit cell volume is encountered before the final (slower) decrease occurs. The same general features are observed at 700°C, where the process is much slower.

So far thermogravimetric experiments have not shown mass variations indicating a two-step oxidation process. The reactions are too fast for *in situ* neutron powder diffraction studies that otherwise could determine the time evolution of the atomic coordinates for the light oxygen atoms. It is presently proposed that the expansion anomaly is caused by redistribution of oxygen vacancies, thereby changing the relative amount of lower coordinated MO_4 tetrahedra and MO_5 square pyramids. Forthcoming *in situ* synchrotron X-ray diffraction experiments will hopefully solve this intriguing problem

Publication: In progress

QEXAFS Study of the Sulfidation of NiMo / Al₂O₃ hydrotreating catalysts

R. Cattaneo, T. Shido & R. Prins

[ETHZ]

The removal of S, N, O and heavy metals is an indispensable step in the refining of petroleum. This hydrotreating process must be improved because of recent stricter legislation concerning the S and N content in oil fractions. In order to optimize the reactivity of the CoMo and NiMo hydrotreating catalysts used in the removal of S and N, a better understanding of the processes used to produce these catalysts is necessary. This study deals with one of the fundamental steps in the preparation of hydrotreating catalysts: presulfiding. Presulfiding is carried out before catalysts are used in hydrotreating reactions in order to convert the oxidic catalyst precursor into the final sulfided catalyst.

Presulfiding consists of heating the catalyst precursor to 673 K in the presence of H₂S. Under these conditions and because of the dynamics of the system, the study must be carried out *in situ*. Quick scanning extended X-ray absorption fine structure (QEXAFS) was used to characterize the various steps in the sulfidation of Mo and Ni in γ -Al₂O₃-supported catalysts.

An investigation of the effect of chelating ligands on the sulfidation of **Mo** as well as of **Ni** is reported. Such ligands improve the hydro-desulfurization (HDS) activity of the catalysts. Our previous work concentrated on the characterization of such modified *NiMo/SiO₂* catalysts in the oxidic and sulfided state.

The main goal of this work was to investigate the influence of chelating ligands on the sulfidation temperature of both Mo and Ni and to learn more about γ -Al₂O₃-supported materials.

The QEXAFS measurements were carried out at the Hamburger Synchrotronstrahlungslabor (HASYLAB) The EXAFS spectra were collected at the Swiss-Norwegian beamlines For both measurements, the catalyst samples were pressed into self-supporting wafers and mounted in an *in situ* EXAFS cell.

In the case of Mo the intermediate product of sulfidation was shown to be a mixture of (MoO₄)⁻² and polymolybdate anions. A survey of various Mo-S compounds pointed to the presence of species similar to (Mo₂S₁₂)⁻² or (Mo₃S₁₃)⁻² (see fig. 4). The final product was MoS₂.

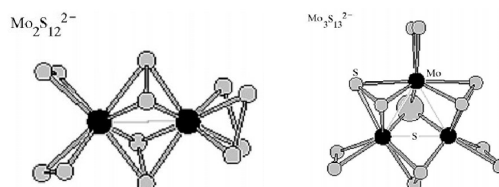


Fig. 4. Structures of (Mo₂S₁₂)⁻² and (Mo₃S₁₃)⁻²

In the case of Ni the QEXAFS spectra recorded during sulfidation showed that the sulfidation mechanisms was strongly affected by the presence of the chelating ligands. The reaction pathway could be deduced by studying the structure of Ni in the final sulfided catalysts. According to EXAFS measurements Ni's parameters showed no similarity to inorganic Ni-S compounds such as Ni₃S₂, NiS or NiS₂; they resembled those of metalorganic trimeric compound bis(dithiobenzoato) nickel (II).

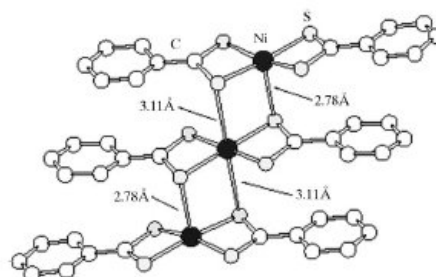


Fig. 5. Structure of trimeric bis(dithiobenzoato) nickel (II)

This suggests that Ni forms small clusters during sulfidation and that it is likely that the chelating agents induce the formation of smaller clusters and consequently a greater dispersion of Ni.

Not one of the less important conclusion drawn from this experiment is that the quantitative information extracted from QEXAFS is limited; this is inherent to the technique (fast data collection produces poor statistics), and this means that to arrive at hard, final conclusions one has to combine this technique with "classical" EXAFS.

Publication: J. Synchr. Rad. 8 (2001) 158–162

Peroxidases: New Resonance Forms Suggested by pH Dependent Structures of Intermediates in Myoglobin-Peroxide Reactions

H.P. Hersleth, B. Dalhus, C. H. Gørbitz & K. K. Andersson

[Oslo]

The main function of myoglobin is storage and transportation of oxygen in muscles, and the haeme group serves as the active site (Fig. 6). Myoglobin can also carry out similar reactions to many peroxidases. The ferric myoglobin reacts with peroxide as shown.

The biological conversions of O_2 and peroxides to water as well as certain incorporations of oxygen atoms into small organic molecules can be catalyzed by metal-ions in different clusters or cofactors. The catalytic cycles of these reactions pass through similar metal-based complexes in which one oxygen or peroxide-derived oxygen atom is coordinated to an oxidized form of the catalytic metal-center.

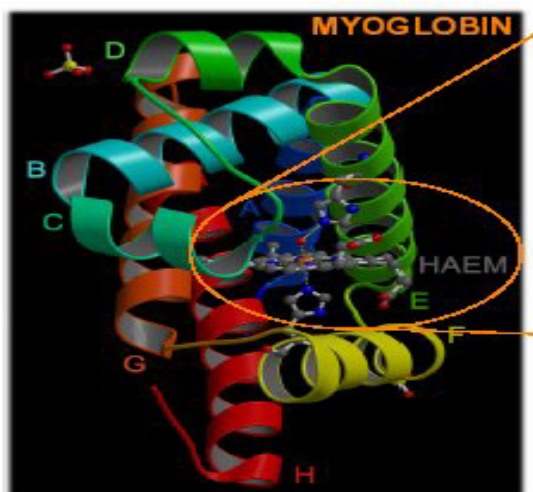


Fig. 6. Myoglobin and its haeme group with the distal and proximal histidines shown. The oxygen atom is an iron-ligated water in the normal metmyoglobin.

In haem-based peroxidases or oxygenases the ferryl ($Fe^{IV}O$) form is important in the

compound I and compound II complexes, which are two and one oxidation equivalents higher than the ferric (Fe^{III}) form, respectively. In this study three high resolution X-ray structures of a compound II model protein are reported, which were obtained by reacting hydrogen peroxide with ferric myoglobin at pH 5.2 (with 1.35 Å resolution), 6.8 and 8.7. The molecular geometry is virtually unchanged compared to the ferric form, indicating that these reactive intermediates do not undergo large structural changes.

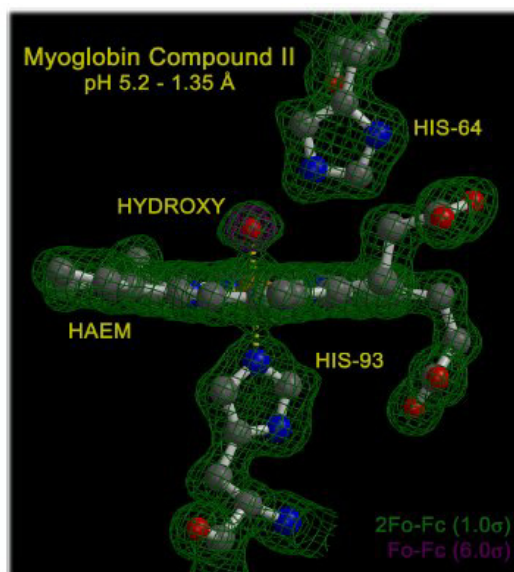


Fig. 7. The haeme site of myoglobin compound II at pH 5.2, with well defined electron density and a strong electron density peak for the oxygen atom.

The small structural changes due to reductive oxygen or peroxide activation of haem proteins should be short-lived and well defined to prevent liberation of reactive oxygen species that might diffuse from the haem binding site,

The essential $Fe\cdots O$ distance is 1.9 Å at all pH-values. This observation, together with the short hydrogen bonding to the distal histidine (2.70 Å), suggests that at low pH the dominant compound II resonance form is a hydroxyl radical-ferric iron and at high pH a hydroxyl-ferryl iron, and not an oxo-ferryl form as has been suggested previously. The 1.9 Å $Fe\cdots O$ distance is in agreement with an EXAFS study of compound II in horseradish peroxidase.

Publication: *J. Biol. Inorg. Chem.* **7** (2002) 299-304

Structure of the charge density wave in $(\text{TaSe}_4)_2\text{I}$

S. van Smaalen, E.J. Lam and J. Luedicke

[Bayreuth]

$(\text{TaSe}_4)_2\text{I}$ is a quasi-one-dimensional (1D) metal, that belongs to the class of $(\text{MX}_4)_x\text{Y}$ compounds ($\text{M} = \text{Ta}, \text{Nb}$; $\text{X} = \text{S}, \text{Se}, \text{Te}$; $\text{Y} = \text{I}, \text{Br}, \text{Cl}$; $x \approx 2$). A characteristic feature of these compounds is the presence of columns of composition MX_4 that are separated by chains of halogenide atoms. $(\text{TaSe}_4)_2\text{I}$ crystallizes in space group $I422$ with lattice parameters $a_0 = b_0 = 9.531 \text{ \AA}$ and $c_0 = 12.824 \text{ \AA}$ at room temperature (fig. 8 and 9). The 1-D electronic properties are presumably related to the 1-D electron band formed by the $5d_{2z}$ orbitals of the Ta atoms.

$(\text{TaSe}_4)_2$ exhibits a phase transition at $T_{CDW} = 263 \text{ K}$ towards a charge-density-wave (CDW) state at low temperatures. We report a full structure refinement of the incommensurately modulated structure in the CDW state at $T = 110 \text{ K}$ against synchrotron radiation, single-crystal x-ray diffraction data. At room temperature the crystal structure has tetragonal symmetry with space group $I422$. In the CDW state each main reflection in the x-ray scattering is surrounded by eight incommensurate satellites at $(\pm 0.064, \pm 0.064, \pm 0.151)$. The CDW state is found to comprise four domains, and it is characterized by one modulation wavevector.

With respect to a $\sqrt{2} \times \sqrt{2} \times 1$ supercell, it has the symmetry of the superspace group $F2(0, \beta, \gamma)$ with $\beta = 0.128$ and $\gamma = 0.151$. The first part of the modulation is found to be a transverse acoustic wave, involving amplitudes of similar magnitudes of about 0.13 \AA on all atoms. The second part of the modulation involves displacements of the Ta atoms of about 0.03 \AA , that are parallel to the 1D chains.

These are interpreted as reflecting the CDW. A Landau free-energy model is developed, that shows that symmetry arguments allow the phase transition to be second order

An anomaly in the temperature dependence of the electrical resistivity was interpreted as being due to the formation of a charge-density wave (CDW) below $T_{CDW} = 263 \text{ K}$.

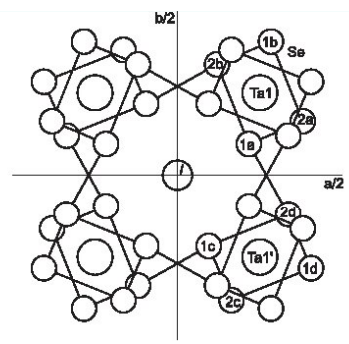


Fig. 8. Projection of the basic structure of one unit cell onto the (a, b) plane. Shown are Ta1 atoms at $z = 0$, iodine atoms at $z = 0.15$, Se atoms at $z = 0.12$. Note that the axes of the F -centred unit cell are indicated.

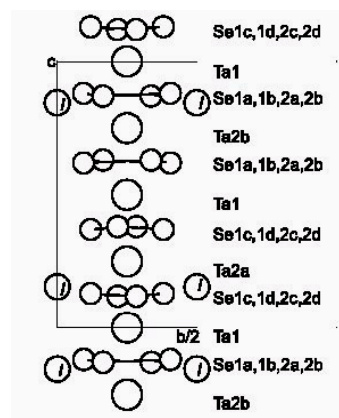


Fig. 9. The structure of the TaSe_4 chain centred on $x = y = 0.25$.

Satellite reflections in x-ray scattering and electron diffraction were observed below T_{CDW} at positions defined by modulation wavevectors $(\pm 0.05, \pm 0.05, \pm 0.09)$, thus supporting the CDW interpretation of the phase transition.

Further evidence for the low-dimensional electronic properties and a CDW state came from angle-resolved photoelectron spectroscopy

Publication: J. Phys. Condens. Matter 13 (2001) 9923-9936

***In situ* characterization of phase transitions in cristobalite under high pressure by Raman spectroscopy and X-ray diffraction**

V.B. Prokopenko , L.S. Dubrovinsky,
V. Dmitriev , H.-P. Weber

[Uppsala, Lausanne and SNBL]

Silica, SiO₂, is a key material in the Earth and materials sciences for a variety of reasons. The high-pressure, high-temperature phases of silica play a significant role in the modeling of geochemical processes in the deep interior of the Earth. In the ceramic industry, its glass phase is of major economic importance.

Of the silica phases studied, quartz, stishovite, coesite and amorphous silica have attracted the most attention so far. Cristobalite, another polymorph of SiO₂, is common in rocks of volcanic origin. Its presence in a rock is helpful to petrologists in determining the temperature of the rock at the time it crystallized.

Cristobalite has a relatively simple structure at ambient conditions, closely related to the diamond structure. At elevated temperature and pressure, however, its structural behaviour appears straightforward at first, but in reality is far more complex. In this study, the structure and optical properties of cristobalite have been studied, *in situ*, under non-hydrostatic pressures of up to 61 GPa, using two different experimental techniques: X-ray powder diffraction and micro-Raman spectroscopy.

The starting material, the α -cristobalite phase of SiO (C-I), was formed from annealing a silica sol-gel glass at 1500°C for 15 min. Mao-Bell and membrane-type diamond anvil cells were used for generation of the high pressure.

On increasing the pressure, four polymorphs were found, both with XRD and micro-Raman spectroscopy: C-I α -cristobalite up to 6 GPa, C-II in the pressure range 0.2–14 GPa, C-III from 14 to 35 GPa, and C-IV above 35 GPa, and no new phase was observed up to 61 GPa. The high-pressure phase C-IV is crystalline, quenchable and clearly different from C-III or from stishovite or other known silica polymorphs.

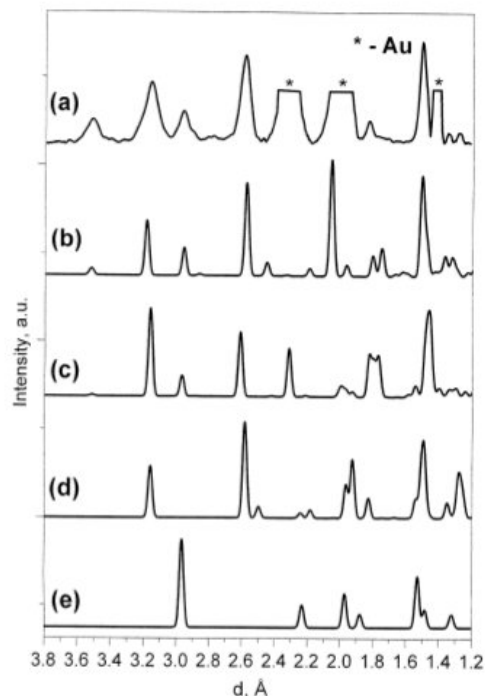


Fig. 10. Comparison of experimental diffraction pattern of decompressed polymorph C-IV at 6.8 GPa (a) with calculated diffraction pattern monoclinically distorted α -PbO₂ (b), a mixture of α -PbO₂ and the distorted monoclinic (P2₁/c) α -PbO₂ (c), an ideal α -PbO₂-type structure (d) and stishovite (e).

The high-pressure phase C-IV is polycrystalline in contrast to earlier reports where amorphization was observed above 30 GPa. A monoclinically distorted α -PbO₂-type structure provides the best fit to the X-ray powder pattern of the recovered phase C-IV (see fig. 10).

It is possible that there is an intermediate phase between C-II and C-III on compression around 14 GPa and on decompression around 8 GPa. This phase is not visible in diffraction spectra, solely in Raman spectra, where it could be associated with the behavior of the disordered silica network or due to an amorphous component.

Publication: J. Alloys & Compounds 327 (2001) 87-95

Catalysis

The goal in research on catalytic materials is a) to search for new such agents, b) to optimize their properties, in particular the rate at which they control chemical reactions, and, ultimately, c) to understand, at the atomic level, the mechanism by which this control is achieved.

Catalysis is of crucial (economic) importance to chemical and biochemical industry. Catalysts come in many forms, from porous solids (such as zeolites) to biological catalysts (such as enzymes). Empirical screening is still an often traveled route in the discovery of new catalysts, and, in many applications, optimization still takes place on an empirical level. It is only in the last quarter century that conclusive experimental techniques to study (and improve) the catalytic mechanism have come to bear; the use of computational techniques is, of course, even more recent. As in many other areas of science, theoretical simulation is used to evaluate materials performance under conditions too difficult or costly to achieve.

Characterization by EXAFS of Co/MFI Catalysts Prepared by Sublimation

V. Schwartz, R. Prins, X. Wang and W.M. H. Sachtler

[ETHZ and Northwestern University]

Zeolite-supported cobalt catalysts are remarkably active in the reduction of nitrogen oxides. Not only do they achieve high conversion of NO_x to N_2 in the presence of a large excess of oxygen, but they are also capable of catalyzing NO_x reduction with methane as the sole reductant. This distinguishes them from zeolite-based catalysts with Cu or Fe as the active ingredient, which require higher alkanes or alkenes as the reducing hydrocarbon. Various techniques have been applied to characterize the cobalt sites in zeolite MFI or ferrierite. It appears that the activity and selectivity of the catalysts critically depends on the metal loading and the technique by which the catalysts were prepared.

In the present case, catalysts have been prepared by subliming CoCl_2 or CoBr_2 vapor onto the H form of the zeolite MFI, followed by replacing the halide ions by OH groups and subsequent heat treatments. The Co sites have been characterized by EXAFS and XANES spectra at liquid nitrogen temperature. The data are correlated with the H_2 -TPR profiles of the same samples and their catalytic performance in reducing NO_x with hydrocarbons. Materials with fairly large Co_3O_4 particles after calcination, displaying a Co-Co distance of 3.5 Å and negligible interaction

between Co and T sites (T = Si or Al), have a poor selectivity in NO_x reduction, because such oxide particles catalyze the combustion of the hydrocarbon. In contrast, highly selective catalysts show no Co_3O_4 clusters and distinct interaction between Co and T atoms. Heating in H_2 at 400 °C reduces Co-oxo ions, while cobalt oxide clusters are incompletely reduced and isolated Co^{2+} ions in exchange positions remain unreduced. The water formed in the reduction of oxo species can interact with Co^{2+} ions, increasing their coordination number with oxygen. A pre-edge XANES peak at 7710 eV indicates an electric-dipole-forbidden, but quadrupole-allowed and vibronically allowed 1s-3d electronic transition.

The present data confirm that calcined Co/MFI samples prepared by sublimation are significantly affected by treatment in H_2 at 400 °C. This distinguishes such catalysts from others that are prepared by ion exchange from aqueous solution and are known to require much higher reduction temperatures.

Treatment in oxygen at 400 °C of the present samples produces oxo species, in which the metal ions are coordinated both with framework and with extraframework oxygen. Accordingly, no data fit is possible by assuming only one set of Co-O distances. The data also indicate that rather large Co_3O_4 clusters were present in the poor catalyst CZO5. This is in line with the previous observations that transition-metal oxide particles possess high activity for the catalytic combustion of hydrocarbons, but a low selectivity for their interaction with N_{ox} .

Publication: J. Phys. Chem. B 106 (2002) 7210-7217

Novel and Unusual Materials

Several of the studies presented below were carried out with more than one experimental technique. This is convincing evidence that at the cutting edge of materials development the use of several experimental probes is essential to answer the questions asked. The SNBL with two basically different experimental techniques (diffraction and absorption), and three different instruments in the field of diffraction, are well placed to contribute to the solution of today's challenging crystallographic problems.

Diffraction anomalous fine structure (DAFS) of forbidden reflection of super-ordered GaInP

L. Alagna, S. Turchini, T. Prosperi
[CNR, Roma]

DAFS is a structural spectroscopic technique suitable to investigate the crystalline structure of domains embedded in a chemically not distinguishable matrix.

Important optical and electronic properties such as birefringence and dichroism result from arrangement of super-ordered domains with uni-axial symmetry, segregated in the solid matrix, and the present work aims at demonstrating that DAFS is the proper technique to structurally characterize such domains. This is a challenging problem as these domains make up only a small percentage of the main system.

In the system under study gallium is present in the substrate as GaAs as well as in the epilayer as InGaP, with the same zinc-blende structure. The epilayer domains of InGaP are expected to have a super-ordered structure, with the zinc-blende cell doubled along the c axis. Hence the forbidden $h/2$ $k/2$ $l/2$ reflection is allowed, and from these extra peaks it ought to be possible to deduct a) from the diffraction profiles size and crystalline quality of the domains in the epilayer and b) from the DAFS spectra short range information around the gallium within the epi-layer of super-ordered domains. The method was first tested on the substrate peaks (GaAs) and on bulk GaP, and then on the allowed reflection of the

InGaP/GaAs epitaxial growth to which InGaP also contributes.

For the allowed reflection the analysis of the EXAFS spectra yielded nearest neighbours of 4 P at 2.4 Å, 6 In at 3.93 Å, 6 Ga at 3.93 Å and 12 P at 4.6 Å.

For the "forbidden" reflection (-5/2, 5/2, -5/2) the DAFS spectrum contains contributions solely from the InGaP super-domains. The best simulation was obtained with distances only slightly different than from InGaP/GaAs, but the striking difference was the presence of a new indium distance at 3.01 Å (see arrow in fig. 11) perfectly the one predicted theoretically for a fully relaxed, near-surface reconstructed structure for neutral InGaP/GaAs (see fig. 11).

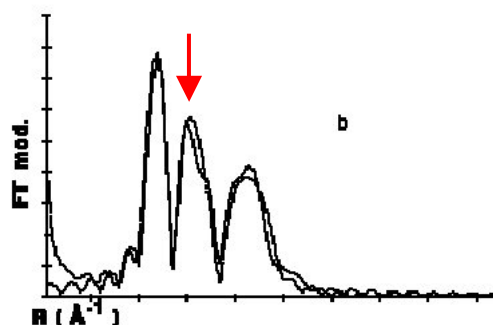


Fig. 11: Fourier transform (solid line) and relative fit (broken line) for DAFS spectrum from forbidden reflection. Only the super-ordered monolayers of InGaP contribute to the data.

Publication: J. Synchr. Rad. 8 (2001) 387-389

Structural Characterization of Solar Cells Prototypes, Based on Nanocrystalline TiO₂ Anatase

Zubavichus, Y.V., Slovokhotov, Y.L., Nazeeruddin, M.K., Zakeeruddin, S.M., Graetzel, M., and V. Shklover

[Moscow, Lausanne & Zurich]

If photosensitive agents such as dyes are sprayed onto nanocrystalline semiconductors, electrons from the photosensitizing molecules (usually compounds with low-lying electron states) are injected into the semiconductor's conduction band under irradiation by visible light. Such dye-sensitized solar cells are a valid and attractive alternative to conventional photovoltaic cells.

In earlier work photo-efficient Ru-containing organic dyes were synthesized. The structures of the dye complexes all included COOH groups, the deprotonation of which at higher pH gives rise to a variety of ionic derivatives. The COOH or COO⁻ groups were expected to anchor the sensitizing molecules to the TiO₂ surface and to play a decisive role in the electron transfer through their π^* -MO during photo-excitation.

The present work aimed at the clarification of this mechanism at the atomic level and in real photovoltaic cells. Experimental evidence was contributed by several techniques, including XRD, XAFS, XPS and electron microscopy.

The x-ray diffraction patterns from these solar cell prototypes, coated with a TiO₂ anatase nanocrystalline film, exhibited broadened anatase reflections corresponding to an average nanocrystallite dimensions of ~12.5 nm. No bulk dye phase was detected. Ti K-edge XAFS data revealed stronger local atomic disorder in the coated samples than in the blank ones. XPS data with consistent with monolayer coating.

Publication: Chem. Mater. 14 (2002) 3556-3563

Note: In the previous annual report one of the Highlights dealt with polymorphism in TiO₂.

Coordination Polymers Constructed from Paddle-Wheel Building Units

Kongshaug, K.O. and H. Fjellvag

[Oslo]

One of the challenges in the field of crystal engineering is to synthesize porous structures capable of selective release and of binding of small molecules. One of the ways to achieve this goal is by designing rigid molecular building units which a) retain their structure when the surrounding framework is dissolved and b) facilitate functionalization of the voids between the building units.

Copper (II) acetate clusters have been known to form such rigid units, with some 340 crystal structures exhibiting this feature. The clusters adopt a paddle-wheel shape (see fig. below) and most frequently link together to 2-D layer structures via aromatic molecules. These sheets are so stacked that 1-D channels form (with dimensions 7 x 16 Å).

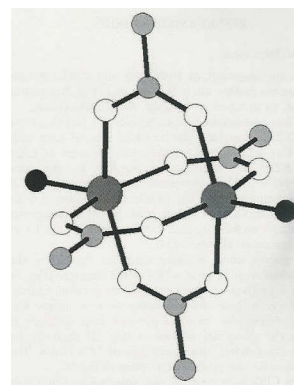


Fig. 12. Paddle-wheel building unit.

Zinc analogs of the copper clusters are also known, although quite rare.

The magnetic properties of these coordination polymers are quite different from compounds containing only discrete paddle-wheel molecules. While in the latter strong antiferromagnetic coupling is observed between the Cu clusters, the coupling between the Cu clusters is weakly ferromagnetic and modulated by the aromatic bridges.

Publication: J. Sol. State Chem. 166 (2002) 213-218

Application of powder diffraction methods to the analysis of the atomic structure of nanocrystals

B.Palosz, E.Grzankai, S.Gierlotka, S.Stel'Makh, R.Pielaszek, U.Bismayer, H.-P. Weber, & W.Palosz

[UNIPRESS, Warsaw; Univ Hamburg; SNBL; Marshall Space Flight Center]

The conventional tools developed for the analysis of powder diffraction data, if applied to diffraction data from nanocrystals, will lead to erroneous interpretation of the experimental results. A different analysis of such diffraction data, based on the so-called "apparent lattice parameter" (*alp*), is being proposed. Nanocrystals are assumed to consist of a core with a well-defined crystal structure, surrounded by a surface shell with an atomic structure similar to that of the core but strained.

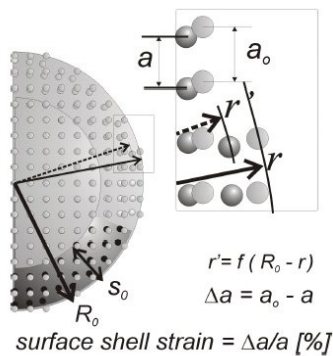


Fig. 13. Model of a nanocrystal with a strained surface layer (R_0 : radius of the core; R : radius of the grain; s_0 thickness of the surface layer; r : distance from the center; a_0 : interatomic distance in relaxed lattice; a_s interatomic distance at the surface).

The two components, the core and the shell, form a composite crystal with interacting and

inseparable diffraction properties. The set of lattice parameters commonly used for the characterization of simple crystal phases is shown to be inappropriate for a proper description of the complex structure of nanocrystals. The model is defined by the lattice parameter of the grain core, thickness of the shell, and the magnitude and distribution of the strain field in the shell, Fig. 13. Strain has considerable effect on diffraction patterns of nanocrystallite as the model shown in fig. 14 demonstrates.

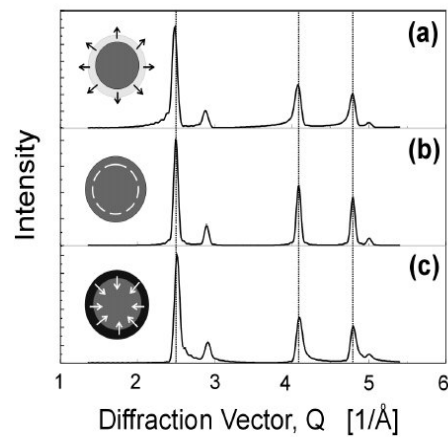


Fig. 14. Diffraction pattern of a 8 nm SiC grain with a surface shell of 0.7 nm thick, and calculated for different magnitude of strain in the surface layer. (a) $Da/a=+10\%$ (b) $Da/a=0\%$ (c) $Da/a=-10\%$.

There are many other effects of crystal size on the diffraction pattern, too numerous to list here.

That the approach and model developed here is correct is demonstrated when one compares theoretical *alp*-*Q* values with those obtained experimentally for real substances such as SiC, GaN, and diamond nanopowders.

Publication: Z. Krist. 217 (2002) 497-509

Magnetic phase transitions in the double spin-chains compound LiCu_2O_2

B. Roessli, U. Staub, A. Amato, D. Herlach, P. Pattison, K. Sablina, G.A. Petrakovskii

[Villigen and SNBL]

One-dimensional $S=1/2$ antiferromagnets have physical properties which can only be accounted for by quantum effects. Compounds with coupled $S=1/2$ chains represent intermediate structures between 1-D and 2-D compounds. In this class of materials, antiferromagnetic long-range order has been observed for compounds with zig-zag chains like SrCuO_2 or with weak inter-chains exchange interactions like Sr_2CuO_3 and Ca_2CuO_3 . A common property of these materials is that both the size of the magnetic moments at saturation and the Néel temperature are strongly reduced due to frustration between exchange integrals and quantum fluctuations.

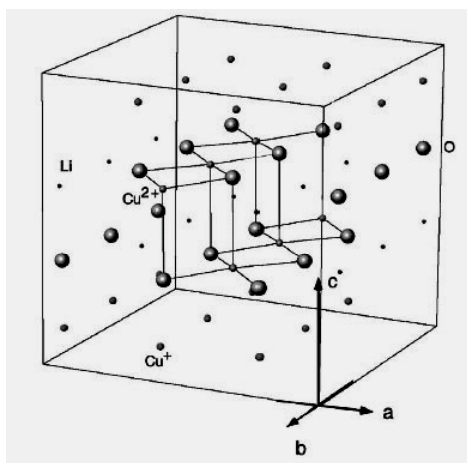


Fig. 15. Structure LiCu_2O_2 , showing the double Cu^{2+} chains.

LiCu_2O_2 is a mixed-valent compound with copper ions in the Cu^{2+} and Cu^{1+} oxidation states. At first the chemical structure of LiCu_2O_2 was described within the tetragonal space group $P4_2/nmc$, then later X-ray and neutron

measurements suggested that LiCu_2O_2 crystallizes at room temperature in the orthorhombic space-group $Pnma$.

The chemical structure of LiCu_2O_2 may be viewed as chains of Cu^{e+} ions propagating along the b-axis (fig. 15). There are two such parallel Cu-chains which run along the a-axis and which are bridged along the c-axis by a 90° oxygen bond. The double-chains are well isolated from each other by both Li-ions and sheets of non-magnetic Cu^{+1} ions.

From these considerations, it appears that LiCu_2O_2 is a good candidate for either a spin-ladder or a zig-zag chain system, depending on the ratio of the nearest- to second-nearest-neighbor exchange interactions.

The goal of this work was to confirm the chemical structure and the origin of the antiferromagnetic ordering, i.e. the magnetic structure.

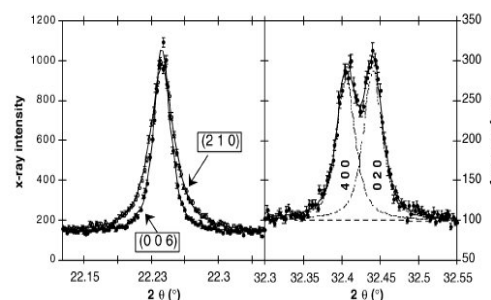


Fig. 16. Anomalous broadening of the (210) Bragg reflection (left); split of (400) and (020) reflections, indicating orthorhombic distortion.

Diffraction experiments with synchrotron radiation revealed that (see fig. 16):

A) Certain classes of diffraction peaks broadened anisotropically, indicating atomic disorder in the (a,b)-plane, i.e. evidence for disorder along the spin chains.

B). At 10K the (400) and (020) reflections are split, a direct and unambiguous evidence that the chemical structure is indeed orthorhombic.

Publication: *Physica B* 296 (2001) 306-311

Rietveld refinement of a chabazite-like aluminophosphate containing a $[\text{Ni}(1,2\text{-diaminoethane})\text{O}_2]^{2-}$ complex bridge

A. Meden, L. McCusker, Chr. Baerlocher, N. Rajic and V. Kaucic

[Ljubljana, Beograd and ETHZ]

Although metal-modified chabazite-like aluminophosphates can be prepared by crystallizing a reactive mixture in the presence of an organic amine, the same procedure cannot be used to synthesize the pure aluminophosphate $\text{AlPO}_4\text{-34}$. Until recently this material has only been prepared in the presence of fluoride ions. Rajic et al. have shown, however, that this aluminophosphate can also be synthesized in the presence of a Ni(II) complex.

This work deals with the structure determination of the as-synthesized form of this $\text{AlPO}_4\text{-34}$ precursor and the interaction between the Ni(II) complex and the aluminophosphate framework. The refined structure turned out to be quite unusual (fig 17). The Ni(II) complex not only exhibits a structure-directing role, but also interacts strongly with the framework. It is not just a template with van der Waals interactions, but an integral part of the framework. Because of the covalent bonding between the complex and P-atoms of the framework, the tetrahedral connectivity of the chabazite framework is

disrupted and full four-connectivity is achieved only after the complex has been removed by calcinations. This is in contrast to the fluoride ions, which form bridges between some Al atoms in a different as-synthesized precursor to $\text{AlPO}_4\text{-34}$.

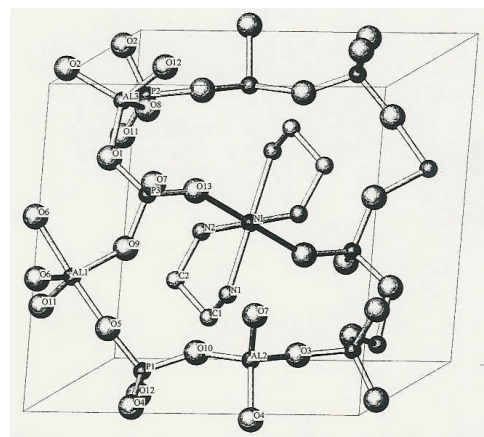


Figure 17. The unit cell of $\text{C}_4\text{H}_{18}\text{N}_4\text{NiAl}_6\text{P}_6\text{O}_{26}$. Some atoms are omitted and their symmetry equivalents from neighboring cells plotted instead to display the connectivity. The atom labels for one asymmetric unit are shown.

Publication: Microporous and Mesoporous Material 47 (2001) 269-274

To keep the facility's instrumentation state-of-the-art and to cope with the increasing complexity of user experiments, upgrades of existing instruments and development of new instruments are being performed continuously, in the background so-to-speak, by SNBL's instrumentation group. Several such improvements were carried out in the past year, and a selection is presented below.

Improvement in Flux Density on Beamlines A and B. Part II.

H. Emerich, W. van Beek and M. Pissard

[SNBL]

The single-most important characteristic of the synchrotron beam from which most users benefit from is the high photon flux that hits the sample. However, flux alone is not sufficient, since the photons must also hit the sample. This implies that:

- the photon beam must be highly focused onto a small area,
- both beam and sample must be accurately positioned and their relative positions maintained in a stable configuration throughout the length of the experiment.

The original goal of the SNBL was to achieve a focal spot size for single crystal experiments of about 0.5 mm diameter and to be able to measure crystals down to about 0.1 – 0.2 mm size. These crystal sizes were typical of synchrotron experiments in macromolecular crystallography in the early part of the 1990's¹. This goal has been met. Although the flux that is being collected cannot be increased, there is, nonetheless, still considerable potential for taking the present focused beam and further reducing the focal spot.

During 1999-2000 SNBL's instrumentation group experimented with (commercially available) focusing capillaries and obtained a gain at the focal spot up to 3 – 4 x, an appreciable improvement. The ideal shape for a focussing capillary is elliptical. However, such a capillary is very difficult to produce and expensive to purchase. For this reason, an idea for a 'new' and improved focussing device was tried. The prototype consisted of two vertically placed pieces of commercial float glass to which a cylindrical shape was given. This very crude set-up already outperformed the commercial capillary by a factor of 2 to 3 x; and so this path was pursued, using a more sophisticated design. Essentially, a mirror was bent such that it adopted an elliptical shape, yielding a working system with an enhancement of the focussed beam's flux density by a factor of 16x (Fig. 18). Another advantage of this device, as compared to a capillary, is that the focal point can be located far away (~15 cm or more) from the beam condenser.

With a size of the x-ray beam of now less than 50 micrometers, i.e. below the resolution of the CCD camera used to image the beam at the sample position, we have encountered another (expected) challenge: Precise sample positioning (down to a few microns). The mechanics for sample alignment on the MAR345 image plate are presently not good enough to align the sample within this very small beam. Once the CCD detector (with its smaller pixel size) is installed on the 6-circle single-crystal diffractometer, we will be able, with better sample positioning mechanics, to fully exploit, at last, our new focusing device.

¹ A typical protein crystal nowadays has a size of 50 μ m in the largest dimension. A narrower beam with a higher flux density but a smaller total integrated flux would obviously be better matched to today's crystal sizes. Smaller sample volumes are encountered not only in protein crystallography, but also in experiments at non-ambient conditions (low and high temperature; high pressure), where the experimental technique imposes the use of unusually minute specimens

Secondary Double Focusing

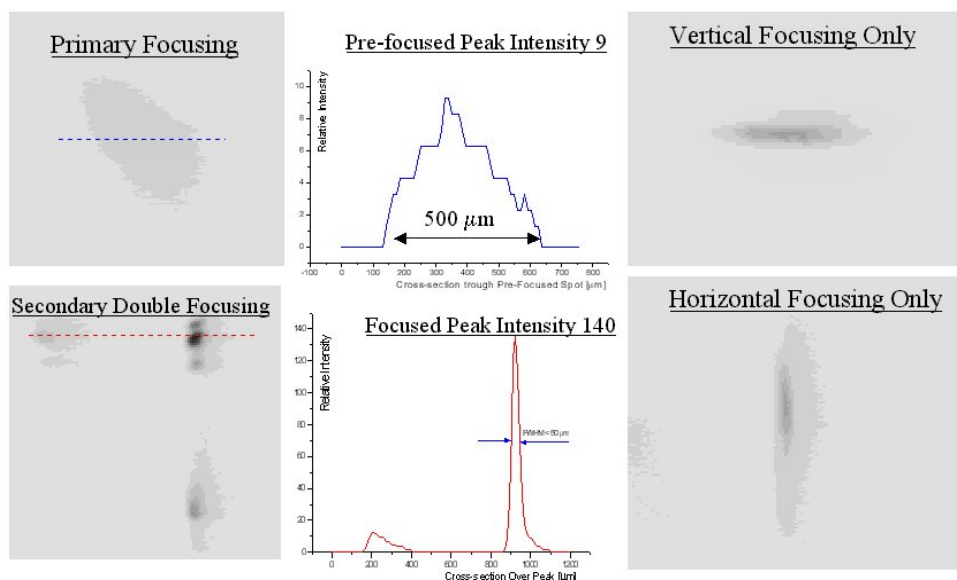


Fig. 18. Focussing the Photon Beam After Monochromator and Mirrors

High-temperature furnace ("micro-reactor")

**H. Emerich, W. van Beek and M.
Pissard**

[SNBL]

Environmental chambers are part of any experimental physical facility. The use of pressure/temperature chambers has a long tradition in XRD; as expected, the advent of synchrotron radiation has led to considerable progress in this kind of instrumentation.

Up to now, the SNBL owned only one single furnace of a design pioneered by the ETHZ Crystallography Laboratory and which fitted the MAR345 area detector. Unfortunately, space limitation prevented its use on the powder diffractometer. Furthermore, and more

importantly, many experiments at high temperature require high-resolution diffraction data, which the MAR345 detector could not provide.

For these reasons, a micro-reactor furnace was developed from an existing, published design. However, in response to wishes from SNBL's users and because of space constraints at the experimental station (powder diffraction branch line), substantial changes were made to the basic concept. The detailed design of the furnace, as well as its construction and testing, was an in-house effort (Fig.18) Tests showed excellent temperature stability, and the temperature gradient over the sample is below 1° at 600°C (Fig. 19)

The sample environment can be pressurized or flushed with inert and oxidizing gazes as well as being put under vacuum; the sample itself can be spun.

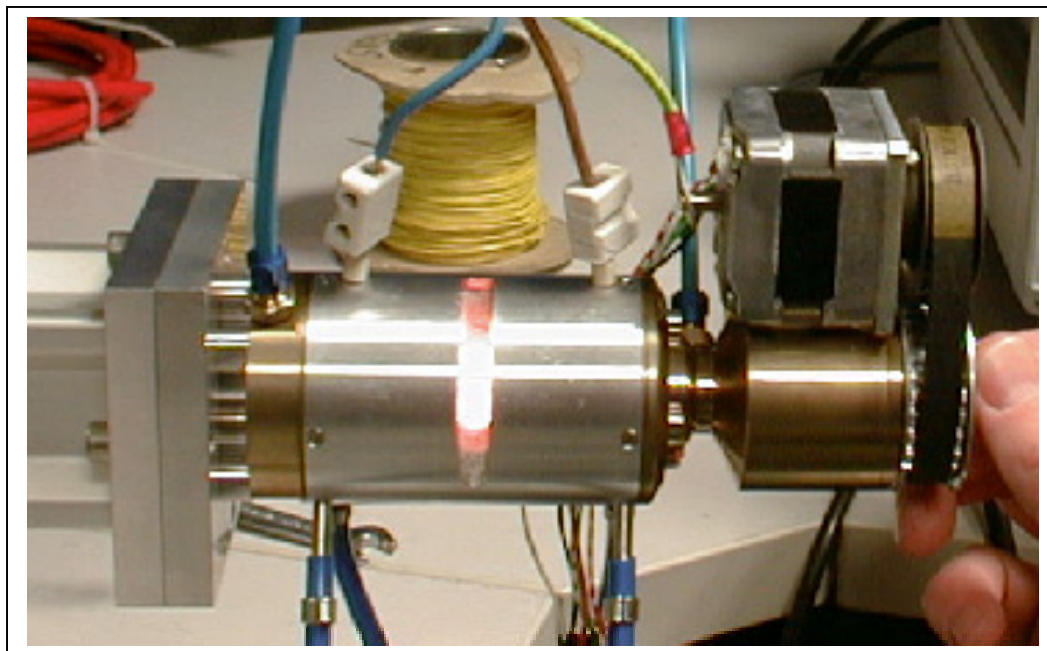


Fig. 19. BL High-temperature Furnace for Powder Diffraction

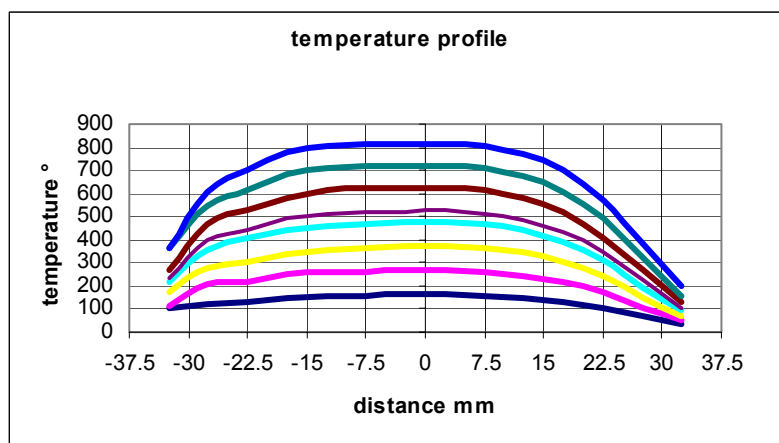


Fig. 20. Temperature Profile

At present the temperature ranges from room temperature up to ~1000°C, but it can be extended up to 1400°C. Control of the temperature is *via* a computer interface. The furnace has now been available for user operation for some months.

Upgrade of Beamline Controls

H. Emerich, W. van Beek and
M. Pissard,

[SNBL]

An advanced facility such as the SNBL cannot afford to stand still and just maintain its equipment. To remain competitive it must continually upgrade hardware and software, and this, to boot, without long-term shutdowns.

B/L control upgrades are just as demanding to implement, if not even more so, than instrument upgrades, but are not as noticeable to the average user (as functionality is often not greatly altered).

One of the major tasks performed over the past year dealt with the replacements of the monochromator's (B/L BM1A) UHV micro-positioners. These micro-positioners align the second crystal in the monochromator with sub-micrometer precision. The old system was taken out and replaced with a new, in-house designed and built one. This meant that all setting parameters, determined during the initial commissioning of the monochromator eight years ago, were lost. The three micro-positioners steer the 0.5*0.5 mm large x-ray beam 25 meters away onto the tiny sample. One can easily imagine that over such a long lever arm alignment is very critical. And so, in order to get the beam out at the other end, one

must be able to track the beam at several points between the monochromator and the sample. Hence three new beam-position monitors were installed. The micro-positioners and beam-position monitors were also embedded into the new control system, making the old control system now fully obsolete.

It should be pointed once more that the average user notices little of the substantial amount of work done behind the scene; except when failure occurs. With the old system, any failure would have been noticed by the user, even before anybody else. With the new system failure is bound to occur much less frequently. The concept is not only technically superior to the old one, in particular it has the advantage of a larger stroke. This opens up the beamlines' capabilities towards higher energies, resulting in, e.g., the ability of collecting higher resolution data (in terms of d-spacing) and having access to a larger number of absorption edges in MAD experiment.

During the past year, many other items were also serviced or changed. Other items included the power electronics for the stepper motors, the air conditioning system for both experimental hutches and people cabins, the beamlines' vacuum pumps (which are being little by little refurbished, giving them a second lease on life), etc.

To the SNBL's credit, all installations/changes have been performed without disruption to user operations.

Fast Time-resolved *in situ* Powder-diffraction Studies

P. Norby, H. Fjellvag and H. Emerich

See Highlight Section of this annual report.

BM1A BRANCH Line

SINGLE CRYSTAL DIFFRACTION – KUMA SIX-CIRCLE DIFFRACTOMETER

The KUMA diffractometer has been used successfully for two projects in which the wavelength tunability of the synchrotron has been exploited to investigate the effects of anomalous scattering and polarization on the diffracted intensities of allowed and forbidden reflections. The application of this technique to protein crystallography is the subject of an experiment in May 2002, which is a collaboration between the University of Lausanne, SNBL and the group of G Bricogne in Cambridge.

The software for the KUMA has been upgraded to a new Windows version and we are currently collecting data with the new software. The group of Frode Mo, for example, measured a total of about 11,000 reflections on the ferroelectric phase of Rochelle salt with an R_{merge} of about 2.5%.

MAR345 AREA DETECTOR

The MAR image plate detector continues to be intensively used both for PX and small molecule crystallography. Successful experiments continue in the fields of high-pressure research and small molecule crystallography. The MAR has proven to be a very versatile instrument, and the latest SNBL proposal rounds for the MAR have been now dominated by non-PX projects.

The He cryo-cooler from Oxford Diffraction has now been delivered. It is possible to install the same cryo-cooler either on the MAR or the KUMA, which opens up some interesting possibilities in low temperature crystallography. An example of data collected on a dipeptide at temperatures of 15K, 100K and 220K demonstrates the advantages of very low temperature data collection in terms of reduced thermal ellipsoids. Low temperature

data sets have also been collected on beta-Ta (Uni Lausanne and SNBL), Trp-Gly.H₂O (SNBL and Uni Lausanne) and Sr₄Ga₈Ge₁₅ (Uni Aarhus and SNBL).

BM1B BRANCH LINE

EXAFS

Till now EXAFS experiments could be carried out in the spectral range from about 6.5 keV at the Mn K-edge to about 40 keV at the Ce K-edge using the Si (111) reflection of the monochromator. By using the Si (333) harmonic from the same monochromator, it is now possible to collect data up to about 48 keV.

We are planning an upgrade of the BM1B monochromator with 2 channel-cut crystals inside the vessel. The 2 monochromators will have different crystal orientation (eg Si 111 and 311) to allow a choice to be made for the energy resolution with rapid change of crystals.

This is important for making XANES scans at high energy around the absorption edge. It is our aim to install the first pair of new crystals at the end of 2002.

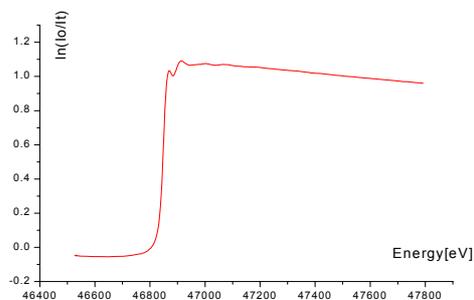


Fig. 21. Sm Edge of Sm₂Co₁₇ in transmission.

Funding has obtained from the Swiss NSF for an upgrade of the EXAFS station, including the purchase of a multi-element detector. The new detector will permit us to extend the range of concentration to more dilute specimens.

The monochromator improvements mentioned above form part of this upgrade.

POWDER DIFFRACTION

The multi-analyzer crystal set-up has been calibrated between about 0.35Å and 1.4 Å, and the data collection time for a full powder pattern at high angular resolution has been reduced to about 6 hours. The cryostat has been often in use, and an in-house furnace (up to 950C) for capillary specimens under controlled atmosphere is now operational.

Both beamlines have also benefited from access to ancillary equipment from the ESRF

loan pool such as sample heaters and special detectors for fluorescence experiments.

OUTLOOK

A further improvement in the productivity and throughput of the beamline can be expected in the coming months. In particular, the use of a CCD area detector in place of the MAR image plate will allow us to collect high quality diffraction data in less than 30 minutes compared to the present time of about 2 – 3 hours (most of which is actually spent reading out the image plate). We will have to make further efforts to improve and streamline the procedures for data analysis, and to support these procedures on the beamline in real-time.

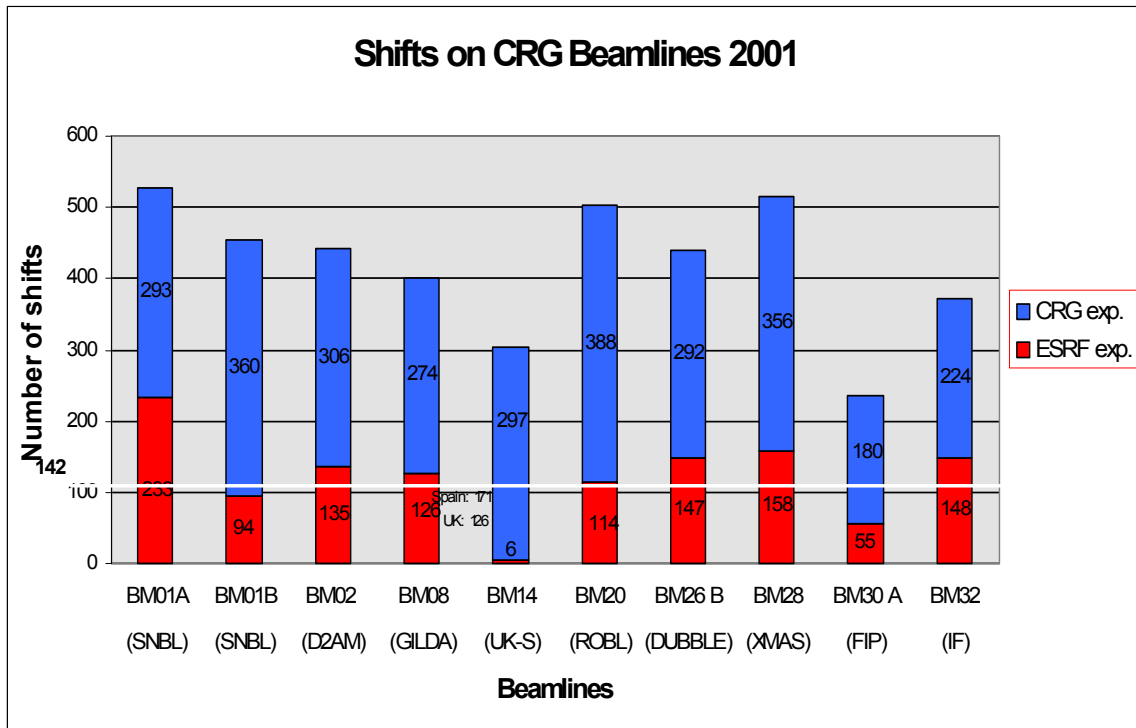


Fig 22. Beamlines statistics: Number of shifts available to users at the different Collaborative Research Group (CRG) beamlines

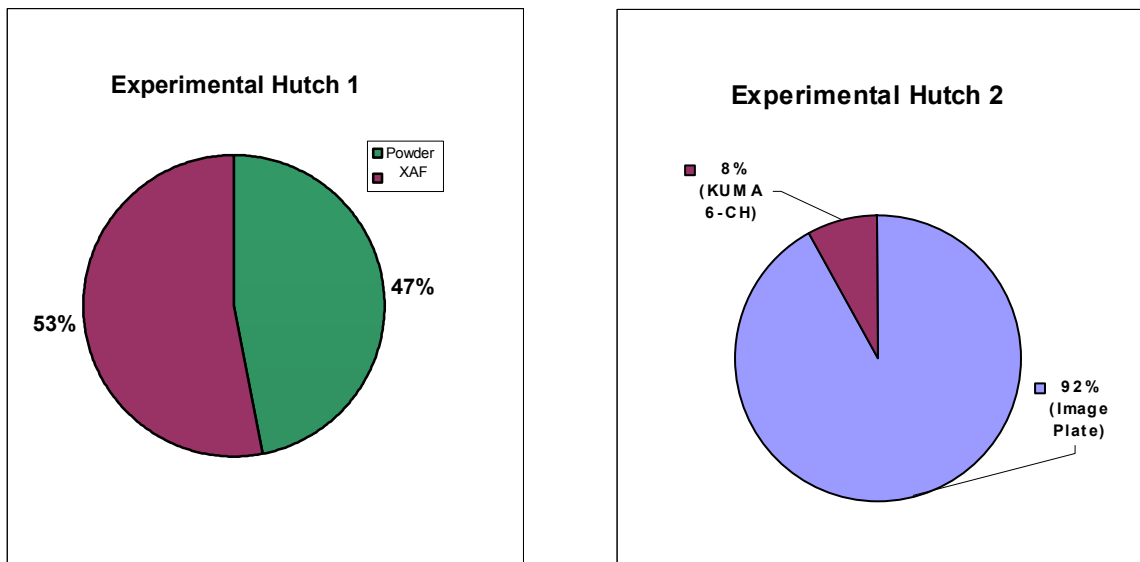


Fig 23. Beamlines statistics: Instrument usage in 2001

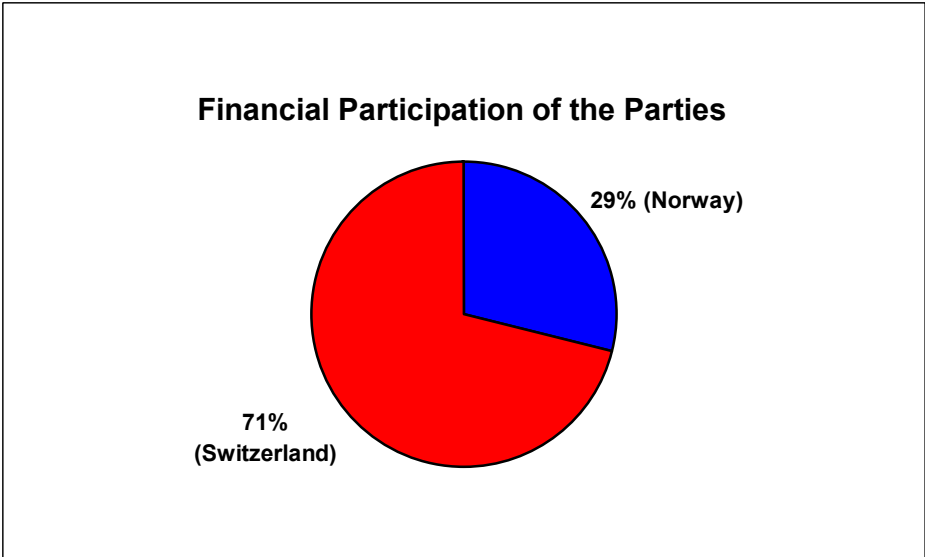


Fig 24. Contribution Share of Each Party (Total funding: CHF 1.24 Mio)

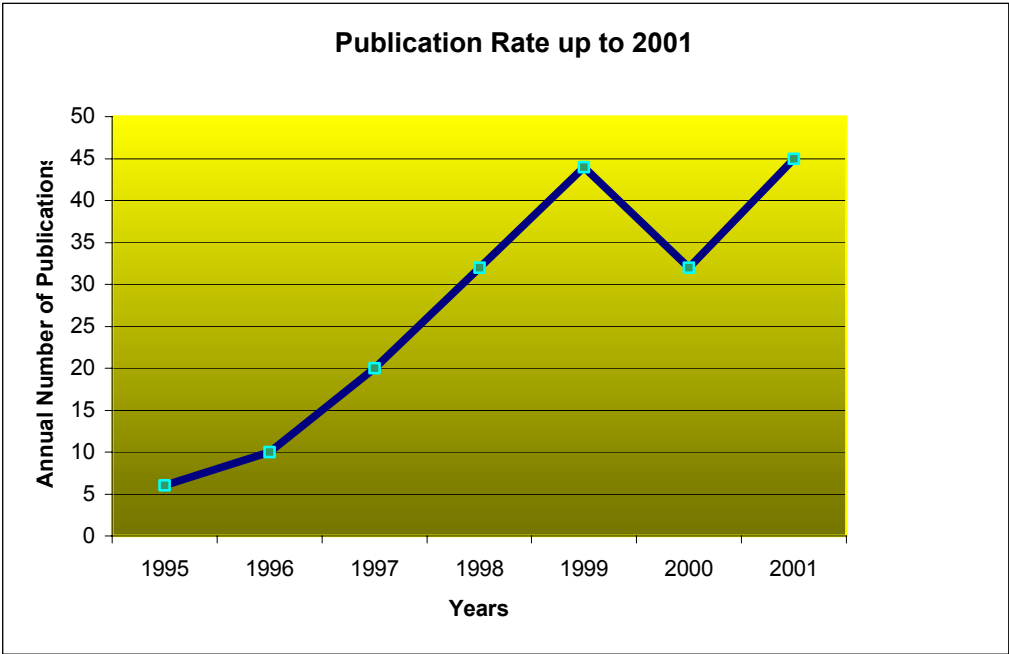


Fig 25. Publication rate since start-up of facility

BEAMLINES PERSONNEL (2000 – 2001)

Hans-Peter Weber	Beamlines Director
Philip Pattison	Beamlines Scientist
Hermann Emerich	Senior Engineer
Wouter van Beek	Engineer
Jon-Are Beukes	Post-doctoral Fellow
Silvia Capelli	Post-doctoral Fellow
Oleksei Kuznetsov	Graduate Student
Chantal Heurtebise*	Executive Assistant
Marc Pissard	Senior Research Technician

* formerly Chantal Seferiadis

STEERING-AND-OVERVIEW COMMITTEE (2000 – 2001)

David Nicholson	Chairperson
Christian Baerlocher	Member
David Banner	Member
Hans-Beat Buergi	Member
Ed Hough	Member
Hans-Peter Weber	Member
Chantal Seferiadis	Secretary
Philip Pattison	Technical Advisor

Experimental and Theoretical Identification of a New High-Pressure TiO₂ Poly

Natalia A. Dubrovinskaia,¹ Leonid S. Dubrovinsky,¹ Rajeev Ahuja,² Vitaly B. Prokopenko,³ V. I. H.-P. Weber,⁴ J. M. Osorio-Guillen,² and Börje Johansson²

¹Bayerisches Geoinstitut, Universität Bayreuth, D-95440 Bayreuth, Germany

²Department of Physics, Uppsala University, S-751 21 Uppsala, Sweden

³Consortium for Advanced Radiation Sources, The University of Chicago, Chicago, Illinois 60637

⁴SNBL, European Synchrotron Radiation Facility, Grenoble 38043, France

(Received 23 March 2001; published 7 December 2001)

Our combined theoretical and experimental investigations have led to the discovery of a new polymorph of titanium dioxide, where titanium is seven-coordinated to oxygen in the orthorhombic OI (*Pbca*) structure. The zero-pressure bulk modulus of the new phase measured in the pressure range 19 to 36 GPa is 318(3) GPa. We demonstrate that the group IVa dioxides (TiO₂, ZrO₂, HfO₂) on compression at ambient temperature all follow the common path: rutile → α-PbO₂-type → baddeleyite-type (MI)

PHYSICA

www.elsevier.com/locate/physb

research p

Crystallographica Section A
Publications of
Crystallography

08-7673

14 July 2000
124 November 2000

Generalized extinction in bipyramidal crystal

G. Thorkildsen,^{a*} H. B. Larsen,^b D. Semmingsen^c and Ø. Bjaanes^b

^aDepartment of Mathematics and Natural Science, Stavanger University College, Ullandhaug, N-4091 Stavanger, Norway, ^bDepartment of Materials Science, Stavanger University College, Ullandhaug, N-4091 Stavanger, Norway, and ^cDepartment of Agriculture and Science, Hedmark University College, N-2322 Ridabu, Norway. Correspondence e-mail: gunnar.thorkildsen@tn.his.no

The generalized extinction factors for a set of strong reflections as a function of wavelength are obtained by indirect measurements. The experiments are performed on a well-defined set of bipyramidal crystals that satisfy the conditions

Physica B 296 (2001) 306–311

Magnetic phase transitions in the double spin-chains compound LiCu₂O₂

B. Roessli^{a,*}, U. Staub^b, A. Amato^c, D. Herlach^c, P. Pattison^d, K. Sablina^e, G.A. Petrakovskii^e

Catalysis 204, 292–304 (2001)

0950-4230/01/\$ - see front matter © 2001 Elsevier Science B.V. All rights reserved.
0950-4230/01/\$18.00, available online at <http://www.idealibrary.com> on IDEAL[®]

Influence of Pretreatment Temperature on the Bimetallic Interactions in Pt-Re/Al₂O₃ Reforming Catalysts Studied by X-Ray Absorption Spectroscopy

Anders Rønning,^{*} Torbjørn Gjervan,^{*} Rune Prestvik,[†] David G. Nicholson,[‡] and Anders

^{*}Department of Chemical Engineering, Norwegian University of Science and Technology (NTNU), N-7491 Trondheim, Norway; [†]SINTEF Applied Chemistry, N-7465 Trondheim, Norway; and [‡]Department of Chemistry, Norwegian University of Science and Technology, N-7491 Trondheim, Norway

doi:10.1006/jmbi.2001.4913 available online at <http://www.idealibrary.com> on IDEAL[®] J. Mol. Biol. (2001) 311, 1037–1048

JMB



Structure of the Soluble Domain of a Membrane-anchored Thioredoxin-like Protein from *Bradyrhizobium japonicum* Reveals Unusual Properties

Guido Capitani^{1,†}, Reinhild Rossmann^{2,†}, David F. Sargent^{3,†}, Markus G. Grütter¹, Timothy J. Richmond³ and Hauke Hennecke^{2*}

¹Biochemisches Institut

TlpA is an unusual thioredoxin-like protein present in the nitrogen-fixing

Influence of pretreatment temperature on the bimetallic interactions in Pt-Re/Al₂O₃ reforming catalysts studied by X-ray absorption spectroscopy

The CD-ROM affixed inside the back cover of this report contains a full bibliography, copies of the first page of every publication as well as all the experimental reports for the past year.

Alagna, L., Turchini, S., Prosperi, T., *Diffraction anomalous fine structure of forbidden reflection of super-ordered GalnP*, J. Synchrotron Rad. **8**, 387-389, 2001

Andersen, O.A., Flatmark, T., Hough, E., *High resolution crystal structures of the catalytic domain of human phenylalanine hydroxylase in its catalytically active Fe(II) form and binary complex with tetrahydrobiopterin*, J. Mol. Biol. **314**, 279-291, 2001

Assarsson, M., Andersson, M.E., Hoegbom, M., Persson, B.O., Sahlin, M., Barra, A.L., Sjoeborg, B.M., Nordlund, P., Graeslund, A., *Restoring proper radical generation by Azide binding to the iron site of the E238A mutant R2 protein of ribonucleotide reductase from Escherichia coli*, J. Biological Chemistry, Vol **276**, N° **29**, 26852-26859, 2001

Birkedal, H., Schwarzenbach, D., Pattison, P., *N-Z-Pro--D-Leu using synchrotron radiation data from a very small crystal*, Acta Cryst. **C57**, 975-977, 2001

Blodig, W., Smith, A.T., Doyle, W.A., Piontek, K., *Crystal Structures of pristine and oxidatively processed lignin peroxidase expressed in Escherichia coli and of the W171F variant that eliminates the Redox Active Tryptophan 171 Implications for the reaction mechanism*, J.Mol.Biol **305**, 851-861, 2001

Brinks, H.W., Yartys, V.A., Hauback, B.C., *Crystal structure of TbNiSiD*, Journal of Alloys & Compounds **322**, 160-165, 2001

Buergi, H-B., Weber, T., *Disorder and motion in crystal structures: nuisance and opportunities*, Chimia **55**, 510-516, 2001

Burton, I.D., Hargreaves, J.S.J., Nicholson, D.G., Nilson, M.H., Stockenhuber, M., *An X-ray absorption study on copper-containing AlPO4-5 for selective catalytic reduction of Nox by propene*, J. Mater.Chem. **11**, 1441-1446, 2001

Capitani, G., Rossmann, R., Sargent, D.F., Gruetter, M.G., Richmond, T.J., Hennecke,

H., *Structure of the soluble domain of a membrane-anchored tioredoxin-like protein from Bradyrhizobium japonicum reveals unusual proterties*, J.Mol.Biol. **311**, 1037-1048, 2001

Cattaneo, R., Shido, T., Prins, R., *QEXAFS study of the sulfidation of NiMo/Al2O3 hydrotreating catalysts*, J. Synchrotron Rad. **8**, 158-162, 2001

Cattaneo, R., Rota, F., Prins, R., *An XAFS study of the different influence of chelating ligands on the HDN and HDS of gamma-Al2O3-supported NiMo catalysts*, J. of Catalysis **199**, 318-327, 2001

Cerny, R., *Powder pattern decomposition with the aid of preferred orientation - Use of the whole Debye-Scherrer Ring*, Materials Science Forum Vols. **378-381**, 24-29, 2001

Dova, E., Goubitz, K., Driessen, R, Sonneveld, E., Chernyshev, V., Schenk, H., *Structure determination of two organometallic complexes from powder data using Grid-Search techniques*, Science Forum Vols **378-381**, 798-802, 2001

Dova, E., Stassen, A.F., Driessen, R.A.J., Sonneveld, E., Goubitz, K., Peschar, R., Haasnoot, J.G., Reedijk, J., Schenk, H., *Structure determination of the [Fe(teec)6](BF4)2 metal complex from laboratory and synchrotron X-ray powder diffraction data with grid-search techniques*, Acta.Cryst. **B57**, 531-538, 2001

Dubrovinskaia, N.A., Dubrovinsky, L.S., Ahuja, R., Prokopenka, V.B., Dmitriev, V., Weber, H-P., Osorio-Guillen, J.M., Johansson, B., *Experimental and theoretical identification of a new high-pressure TiO2 polymorph*, Physical Review Letters, Vol.**87**, N° 27, 275501-1/4, 2001

Fauth, F., Suard, E., Caignaert, V., *Intermediate spin state of Co3+ and Co4+ ions in La0.5Ba0.5CoO3 evidenced by Jahn-Teller distortions*, Phys. Review B, Vol **65**, 060401-060404, 2001

Fjellvag, H., Akporiaye, D.E., Halvorsen,

- E.N., KarlsSon, Arne, Kongshaug, K.O., Lillerud, K.P.**, *Crystal structure and MAS-NMR study of rehydrated UiO-7*, *Solid State Science* **3**, 603-611, 2001
- Flavell, W.R., Nicholson, D.G., Nilsen, M.H., Stahl, K.**, *X-ray powder diffraction and EXAFS studies on SnAPO-5 and Cu:SnAPO-5*, *J. Mater.Chem.* **11**, 620-627, 2001
- Franceschi, F., Guillemot, G., Solari, E., Floriani, C., Re, N., Birkedal, H., Pattison, P.**, *Reduction of Diosygen by a Dimanganese Unit Bonded Inside a Cavity Provided by a Pyrrole-Based Dinucleating Ligand*, *Chem. Eur. J.* **7** No.7, , 2001
- Hege, T., Efeltzer, R.E., Gray, R.D., Baumann, U.**, *Crystal structure of a complex between Pseudomonas aeruginosa alkaline protease and its cognate inhibitor*, *J. Biol.Chemistry* **276**, N° 37, 35087-35092, 2001
- Hege, T., Baumann, U.**, *Protease C of Erwinia Chrysanthemi: The Crystal Structure and role of amino acids Y228 and E189*, *J. Mol. Biol.* **314**, 187-193, 2001
- Hensen, E.J.M., Kooyman, P.J., Van der Meer, Y., Van der Kraan, A.M., de Beer, V.H.J., Van Veen, J.A.R., Van Santen, R.A.**, *The relation between morphology and hydrotreating activity for supported MoS2 particles*, *J. of Catalysis* **199**, 224-235, 2001
- Hersleth, H.P., Dalhus, B., Bgoerbitz, C.H., Andersson, K.K.**, *An iron hydroxide moiety in the 1.35Å resolution structure of hydrogen peroxide derived myoglobin compound II at pH 5.2*, *J. Bio. Inorg. Chem.*, **7** (3), 299-304, 2001
- Hilge M., Perrakis A., Abrahams JP., Winterhalter, K., Piontek K., Gloor SM.**, *Structure elucidation of beta-mannanase: From the electron-density map to the DNA sequence*, *Acta Crystal.* **D57**, 37-43, 2001
- Hoegbom, M., Andersson, M.E., Nordlund, P.**, *Crystal structures of oxidized dinuclear manganese centres in Mn-substituted class I ribonucleotide reductase from Escherichia coli: carboxylate shifts with implications for O2 activation and radical generation*, *J. Biol. Inorg. Chem.*, **6**, 315-323, 2001
- Hostettler, M., Birkedal, H., Schwarzenbach, D.**, *Polymorphs and structures of mercuric iodide*, *Chimia* **55**, 541-545, 2001
- Kongshaug, K.O., Fjellvaeg, H., Lillerud, K.P.**, *The synthesis and characterization of a new manganese phosphate templated by piperazine*, *J. of Solid State Chemistry* **156**, 32-36, 2001
- Kostrewa, D., D'Arcy, A., Takacs, B., Kamber, M.**, *Crystal structures of Streptococcus pneumoniae N-acetylglucosamine-1-phosphate uridyltransferase, GlmU, in Apo form at 2.33 Å resolution and in complex with UDP-N-acetylglucosamine and Mg2+ at 1.96 Å resolution*, *J. Mol. Biol* **305**, 279-289, 2001
- Leiros, I., Lanes, O., Sundheim, O., Helland, R., Smalas, A.O., Willassen, N.P.**, *Crystallization and preliminary X-ray diffraction analysis of a cold-adapted uracil-DNA glycosylase from Atlantic cod (Gadus morhua)*, *Acta. Cryst.* **D57**, 1706-1708, 2001
- Marturano, P., Drozdovaa, L., Pirngruber, G.D., Kogelbauer, A., Prins, R.**, *The mechanism of formation of the Fe species in Fe/ZSM-5 prepared by CVD*, *Phys. Chem. Chem. Phys.* **3**, 5585-5595,
- Meden, A., McCusker, L.B., Baerlocher, C., Rajic, N., Kaucic, V.**, *Rietveld refinement of a chabazite-like aluminophosphate containing a [Ni(1,2-diaminoethane)2O2]2- complex bridge*, *Microporous and Mesoporous Materials* **47**, 269-274, 2001
- McCusker, L. B., Baerlocher, C., Grosse-Kunstleve, R., Brenner, S., Wessels, T.**, *Solving complex zeolite structures from powder diffraction data*, *Chimia* **55**, 497-504, 2001
- Olafsen, A., Larsson, A-K., Fjellvag, H., Hauback, B.C.**, *On the Crystal Structure of Ln2O2CO3II(Ln=La and Nd)*, *J. of Solid State chemistry*, **158** (1), 14-24, 2001
- Patterson, B.D., Abela, R., Van der Veen, F.**, *Materials science at the Swiss Light Source*, *Chimia* **55**, 534-540, 2001
- Prokopenko, V.D., Dubrovinsky, L.S., Dmitriev, V., Weber, H-P.**, *In situ characterization of phase transitions in cristobalite under high pressure by Raman spectroscopy and X-ray diffraction*, *J. of Alloys and Compounds* **327**, 87-95, 2001
- Ramaswamy, V., Tripathi, B., Srinivas, D., Ramaswamy, A.V., Cattaneo, R., Prins, R.**, *Structure and redox behavior of zirconium un microporous Zr-silicalites studied by EXAFS and ESR techniques*, *J. of Catalysis* **200**, 250-258, 2001
- Renaudin, G., Fischer, P., Yvon, K.**, *Tetragonal structure of neodymium deuteride NdD2.27 revisited*, *J. of Alloys and*

Compounds **329**, L9-L13, 2001

Roening, M., Gjervan, T., Prestvik, R., Nicholson, D.G., Holmen, A., *Influence of pretreatment temperature on the bimetallic interactions in Pt-Re/Al₂O₃ reforming catalysts studied by x-ray absorption spectroscopy*, Journal of Catalysis **204**, 292-304, 2001

Roessli, B., Staud, U., Amato, A., Herlach, D., Pattison, P., Sablina, K., Petrakovskii, G.A., *Magnetic phase transitions in the double spin-chains compound LiCu₂O₂*, Physica **B 296**, 306-311, 2001

Steurer, W., Cervellino, A., Lemster, K., Ortelli, S., Estermann, M.A., *Ordering principles in decagonal Al-Co-Ni quasicrystals*, Chimia **55**, 528-533, 2001

Thorkildsen, G., Larsen, H.B., Semmingsen, D., Bjaanes, O., *Generalized extinction in bipyramidal crystals*, Acta. Crystal. **A57**, 201-

211, 2001

Van Langevelde, A., Peschar, R., Schenk, H., *Structure of B-trimyristin and B-tristearin from high-resolution X-ray powder diffraction data*, Acta. Crystal. **B57**, 372-377, 2001

Van Smaalen, S., Lan, E.L., Luedecke, J., *Structure of the charge density wave in (TaSe₄)₂I*, J. Phys. Condens.Matter **12**, 9923-9936, 2001

Weber, T., Estermann, M.A., Buerger, H-B., *Structural complexity of a polar perhydrotriphenylene inclusion compound brought to light by synchrotron radiation*, Acta. Cryst **B57**, 579-590, 2001

Ziegler, F., Scheidegger, A.M., Johnson, C.A., Daehn, R., Wieland, E., *Scorpion mechanisms of zinc to calcium silicate hydrate: x-ray absorption fine structure (XAFS) investigation*, Environ. Sci. Technol. **35**, 1550-1555, 2001

**THE SWISS -
NORWEGIAN
BEAMLINES
AT ESRF**

